Karlsruher Institut für Technologie

Convergence of an adaptive *hp* finite element strategy in higher space-dimensions

M. Bürg
W. Dörfler

Preprint Nr. 10/06

INSTITUT FÜR WISSENSCHAFTLICHES RECHNEN
UND MATHEMATISCHE MODELLBILDUNG

Anschriften der Verfasser:

Dipl.-Math. Markus Bürg
Institut für Angewandte und Numerische Mathematik
Karlsruher Institut für Technologie (KIT)
D-76128 Karlsruhe

Prof. Dr. Willy Dörfler
Institut für Angewandte und Numerische Mathematik
Karlsruher Institut für Technologie (KIT)
D-76128 Karlsruhe

Convergence of an adaptive *hp* finite element strategy in higher space-dimensions

M. Bürg*, W. Dörfler

Karlsruhe Institute of Technology, Department of Mathematics, D-76128 Karlsruhe

Abstract

We show convergence in the energy norm for an automatic *hp*-adaptive refinement strategy for finite elements on the elliptic boundary value problem. The result is a generalization of a marking strategy, which was proposed in one space-dimension, to problems in two- and three-dimensional spaces.

Keywords: adaptive mesh refinement, a posteriori error estimates, convergence, *hp* version of the finite element method

1. Introduction

The finite element method is a widely accepted tool for the numerical solution of partial differential equations. Nowadays a posteriori error estimation is an expected and assessed feature in scientific computing. It is used for adaptively creating approximation spaces and to assess the accuracy of numerical solutions. The performance of the method can be improved by mesh refinement (h-refinement) or the use of higher order ansatz spaces (p-refinement). Taking a combination of both (hp-refinement) can lead to exponentially fast convergence with respect to the number of degrees of freedom [19]. For the h-FEM adaptive mesh creation is discussed in e. g. [1, 23]. For the p- and hp-FEM several strategies have been proposed to create problem-dependent meshes adaptively. There are a lot of different approaches to decide whether it is favourable to increase the polynomial degree p or to decrease the mesh size h. E. g. in [9, 13] the analyticity of the solution is estimated, in [2, 8, 12] local boundary value problems are solved and in [6, 18] the global interpolation error is minimized.
In this paper we generalize the refinement strategy proposed in [8] to problems in two and three space-dimensions and present numerical results of the application of this refinement strategy to some representative problems.
The paper is organized as follows: In Section 2 we state some general assumptions and introduce the model problem. In Section 3 we develop the refinement strategy for two- and three-dimensions and prove its convergence in two space-dimensions explicitly. Further we give numerical results of the application of our refinement strategy to some examples of the model problem in Section 4.

2. Preliminaries

In this section we give the notations and general assumptions, which we will use throughout this paper. Further we state the model problem, which we will consider here.

*Corresponding author
Email addresses: buerg@kit.edu (M. Bürg), willy.doerfler@kit.edu (W. Dörfler)

2.1. Notations and Assumptions

For $d = 1, 2, 3$ let $\Omega \subset \mathbb{R}^d$ be an open domain with polygonal boundary. By $L^2(\Omega)$ and $H_0^1(\Omega)$ we denote as usual the Lebesgue space of square-integrable functions in Ω respectively the Sobolev space of functions in $H^1(\Omega)$ with homogeneous Dirichlet boundary. By $\mathcal{K}$ we denote a triangulation of Ω.
Throughout this paper we assume that $\mathcal{K}$ satisfies the following regularity property [19, 22].

Definition 1 (Shape regularity)**.** *Let $K \in \mathcal{K}$ be the image of the reference cell $\widehat{K}$ under some affine map $F_K : \widehat{K} \mapsto K$. Set $h_K := \operatorname{diam}(K)$. Then $\mathcal{K}$ is called* γ-shape regular*, if and only if there exists some $\gamma > 0$ such that*

$$\frac{\|\nabla F_K\|_{L^\infty(\widehat{K})}}{h_K} + h_K \|(\nabla F_K)^{-1} \circ F_K\|_{L^\infty(\widehat{K})} \leq \gamma \qquad \forall K \in \mathcal{K}.$$

Let $K \in \mathcal{K}$ be arbitrary. Then we set

$$\omega_{K,1} := K \cup \{x \in L : L \in \mathcal{K},\ K \text{ and } L \text{ have a common edge}\}$$

and for $i > 1$ we inductively define

$$\omega_{K,i} := \bigcup_{\substack{K \in \mathcal{K} \\ K \cap \omega_{K,i-1} \neq \emptyset}} K.$$

For simplicity we will write $\omega_K := \omega_{K,1}$. Let $p := (p_K)_{K \in \mathcal{K}}$, $p_K \in \mathbb{N}$, be the polynomial degree vector on mesh $\mathcal{K}$. Then we set

$$p_{\omega_K} := \max_{L \subset \omega_K} (p_L),$$

where p_L denotes the polynomial degree of the ansatz space on cell L. Let $f \in L^2(\Omega)$ and $q \in \mathbb{N}$ be arbitrary. Then we denote the local L^2-projection of f onto the space of polynomials of degree q by f_q. For $d \in \{1, 2, 3\}$ let $Q := [0, 1]^d$ be the reference square respectively the reference cube and

$$T := \left\{ x \in \mathbb{R}^d \,:\, 0 < x_1, \ldots, x_d,\ \sum_{i=1}^{d} x_i \leq 1 \right\}$$

be the reference d-simplex. Obviously we have $Q = T$ for $d = 1$. Let

$$S_0^p(\mathcal{K}, \Omega) := \left\{ u \in H_0^1(\Omega) \,:\, u|_K \circ F_K \in P_{p_K}\left(\widehat{K}\right)\ \forall K \in \mathcal{K} \right\}$$

be a finite dimensional approximation space of piecewise polynomials with homogeneous Dirichlet boundary, where

$$P_p\left(\widehat{K}\right) = \begin{cases} \operatorname{span}\{x^i y^j : 0 \leq i, j \leq p\}, & \text{if } \widehat{K} = Q \\ \operatorname{span}\{x^i y^j : 0 \leq i + j \leq p\}, & \text{if } \widehat{K} = T \end{cases}.$$

Finally, for $N \in \mathbb{N}$ we denote the mesh after refinement step N by $\mathcal{K}_N$.

2.2. The Model Problem

Throughout this paper we consider the problem to find $u : \Omega \to \mathbb{R}$ such that

$$\begin{aligned} -\Delta u &= f \quad \text{in } \Omega, \\ u &= 0 \quad \text{on } \partial\Omega \end{aligned} \tag{1}$$

for given $f : \Omega \to \mathbb{R}$. Multiplying the first equation of problem (1) with $\phi \in H_0^1(\Omega)$ and integrating by parts yields the *weak formulation*

$$\int_\Omega (\nabla\phi)^T \nabla u = \int_\Omega \phi f \qquad \forall \phi \in H_0^1(\Omega). \tag{2}$$

If $f \in L^2(\Omega)$, then the Lax–Milgram Theorem states that there exists a unique $u \in H_0^1(\Omega)$ satisfying (2). Analogously, the discrete problem reads: Find $u_N \in S_0^p(\mathcal{K}_N, \Omega)$ such that

$$\int_\Omega (\nabla\phi_N)^T \nabla u_N = \int_\Omega \phi_N f \qquad \forall \phi_N \in S_0^p(\mathcal{K}_N, \Omega) \tag{3}$$

for given $f \in L^2(\Omega)$.

Remark 1 (Nonhomogeneous boundary conditions)**.** *For problems with nonhomogeneous Dirichlet boundary conditions $u = g$ on $\partial\Omega$, where $g : \partial\Omega \to \mathbb{R}$, we may simply assume that there exists a lifting $u_g \in H^1(\Omega)$ satisfying $u_g = g$ on $\partial\Omega$ such that this solution u is given by $u := u_0 + u_g$, where u_0 is the solution of the homogeneous boundary value problem* (1)*.*

3. *hp*-Adaptive Refinement Strategy

In this section we present our refinement strategy for problems in two and three space-dimensions and prove the convergence of this *hp*-adaptive algorithm for two space-dimensions explicitly.

3.1. Refinement Strategy

The refinement strategy, which we present here, was developed in [8] for one space-dimension. In this section we present a modified formulation, which is applicable to problems in two and three space-dimensions as well.

Let TOL > 0 be some prescribed tolerance for our computed solution. We start our algorithm with some coarse decomposition $\mathcal{K}_0$ of Ω and the approximation space $S_0^p(\mathcal{K}_0, \Omega) \subset H_0^1(\Omega)$. We solve the discrete problem (3) on this initial discretization and check if the energy error is below the prescribed tolerance.

3.1.1. Energy error indicator

We will estimate the energy error a posteriori, that is, only knowing the discrete solution u_N and data. For two dimensions the following method was proposed in [16]:

Definition 2 (Residual error estimator)**.** *Let $K \in \mathcal{K}_N$ be arbitrary, h_K its diameter and p_K the polynomial degree on the cell. Then the* residual error indicator *η_K associated with element K is given by $\eta_K^2 = \eta_{R,K}^2 + \eta_{B,K}^2$, where*

$$\eta_{R,K} := \frac{h_K}{p_K} \| f_{p_K - 1} + \Delta u_N \|_{L^2(K)}$$

is the weighted residual *on cell K and*

$$\eta_{B,K}^2 := \sum_{f \subseteq \partial K \cap \Omega} \frac{h_f}{2p_f} \left\| \left[\frac{\partial u_N}{\partial n_f} \right] \right\|_{L^2(f)}^2$$

is the weighted boundary residual *with n_f denoting the outward pointing unit normal and $[w]$ denoting the* jump *of a function w over face f.*

3.2. Refinement Patterns

A local procedure to enhance the finite element space is called a *refinement pattern*. For the h-adaptive FEM the common refinement pattern to choose is the equal-sized bisection in every coordinate-direction. To reduce the error contribution of the boundary terms as well, we have to assure that no new hanging-nodes are produced at the edges of the cell. Thus we also have to refine the neighboring cells at least anisotropically. This is shown for a quadrilateral in Figure 1 on the left-hand side. For the p-adaptive FEM the common choice is to increase the polynomial degree p_K by one, see Figure 1 on the right-hand side. Also in this case we have to make sure that no new constrained degrees of freedom are created. Hence we increase the polynomial degree on the neighboring cells as well. Further we provide the choice of increasing the polynomial degree by two in some applications. This is shown in Figure 2. Thus for the hp-adaptive FEM we have at least two different refinement patterns, the bisection and the increment of the polynomial degree. Of course there are much more refinement patterns, which can be applied here, e. g. anisotropic h-refinement or the increment of the polynomial order by some arbitrary number. Henceforth let us assume that we have $n \in \mathbb{N}$, $n \geq 2$, different refinement patterns to choose from.

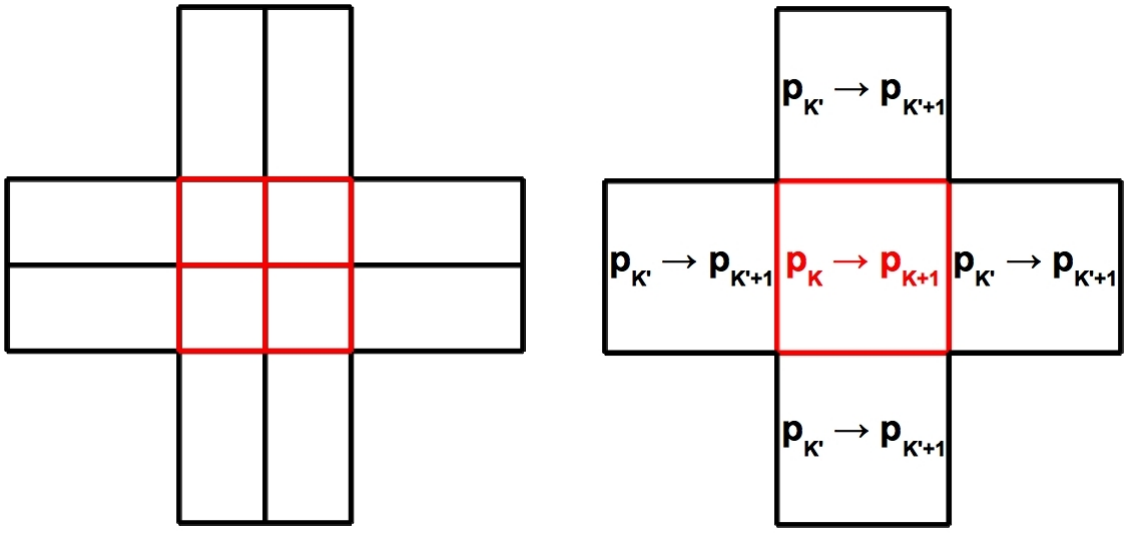

Figure 1: Refinement patterns on cell K. Left: Bisection in x- and y-direction. Right: Increase polynomial degree by one.

3.2.1. Convergence indicators for refinement cases

Let $j \in \{1, \ldots, n\}$ and $K \in \mathcal{K}_N$ be arbitrary. Then we denote the finite element space of functions compactly supported in ω_K with refinement pattern j applied to K by $S^p_{0,K,j}(\mathcal{K}_N, \omega_K)$. Let $\beta_{K,j}$ be the solution of the optimization problem

$$\beta_{K,j}\eta_K = \sup_{\phi \in S^p_{0,K,j}(\mathcal{K}_N,\omega_K)} \left(\frac{\int_{\omega_K} (\phi f_{p_{\omega_K}} - (\nabla\phi)^T \nabla u_N)}{\|\nabla\phi\|_{L^2(\omega_K)}} \right). \tag{4}$$

If $v_{N,j} \in S^p_{0,K,j}(\mathcal{K}_N, \omega_K)$ is the solution of the problem

$$\int_{\omega_K} (\nabla\phi)^T \nabla v_{N,j} = \int_{\omega_K} (\phi f_{p_{\omega_K}} - (\nabla\phi)^T \nabla u_N) \qquad \forall \phi \in S^p_{0,K,j}(\mathcal{K}_N, \omega_K),$$

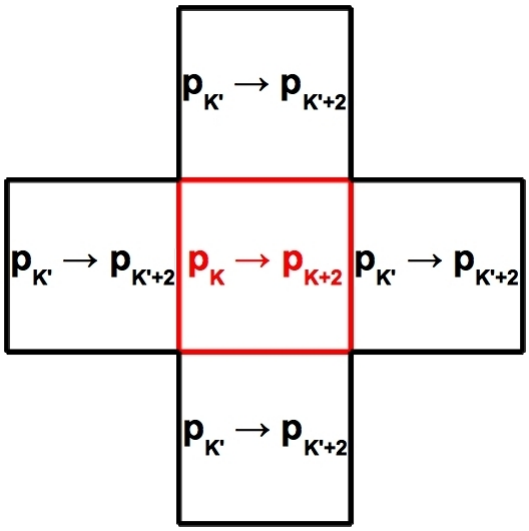

Figure 2: Increase polynomial degree by two.

then we can see that for all $\phi \in S^p_{0,K,j}(\mathcal{K}_N, \omega_K)$

$$\frac{\int_{\omega_K}(\phi f_{p_{\omega_K}} - (\nabla\phi)^T \nabla u_N)}{\|\nabla\phi\|_{L^2(\omega_K)}} \leq \frac{\int_{\omega_K}(v_{N,j} f_{p_{\omega_K}} - (\nabla v_{N,j})^T \nabla u_N)}{\|\nabla v_{N,j}\|_{L^2(\omega_K)}} = \|\nabla v_{N,j}\|_{L^2(\omega_K)}.$$

Thus $v_{N,j}$ is the solution of the optimization problem.

3.2.2. Marking cells for refinement

Hence, if we solve problem (4) for every refinement case, we have a guess which refinement case provides the biggest error reduction on every cell. Unfortunately this is not enough, because simply heading for the biggest error reduction might be inefficient. Thus we also would like to take into account the amount of work required for the achieved reduction of the error. For this we define numbers $w_{K,j}$ to be the number of degrees of freedom, which the local refinement space $S^p_{0,K,j}(\mathcal{K}_N, \omega_K)$ has after we applied refinement pattern j to cell K. Then we can mark the cells for refinement by looking for a solution $\left(\mathcal{A}_N, (j_K)_{K\in\mathcal{A}_N}\right)$ of the minimization problem

$$\sum_{K\in\mathcal{A}_N} \frac{w_{K,j_K}}{\beta_{K,j_K}} = \min \tag{5}$$

under the constraint

$$\sum_{K\in\mathcal{A}_N} \left(\beta_{K,j_K}\varepsilon_K\right)^2 \geq \theta^2 \sum_{K\in\mathcal{K}_N} \varepsilon_K^2. \tag{6}$$

Unfortunately this problem is NP-hard. Here we suggest the following strategy: First we define $j_K \in \mathbb{N}$ for every $K \in \mathcal{K}_N$ by

$$\frac{w_{K,j_K}}{\beta_{K,j_K}} = \min_{j=1,\ldots,n} \left(\frac{w_{K,j}}{\beta_{K,j}}\right)$$

and then we construct a minimal possible $\mathcal{A}_N$ fulfilling constraint (6) as proposed in [7].

3.2.3. hp-adaptive refinement algorithm

In summary, we can state our *hp*-adaptive refinement algorithm as follows:

(S0) Start with coarse grid $\mathcal{K}_0$, $N := 0$.

(S1) Solve the linear system of equations to get an approximate solution $u_N \in S_0^p(\mathcal{K}_N, \Omega)$.
Compute a local error indicator ε_K on every cell $K \in \mathcal{K}_N$.
If

$$\varepsilon^2 := \sum_{K \in \mathcal{K}_N} \varepsilon_K^2 > \text{TOL} :$$

For all cells $K \in \mathcal{K}_N$ and all refinement cases $j = 1, \ldots, n$ compute the values $\beta_{K,j}$ as shown in Section 3.2.1.
Else: STOP

(S2) To mark the cells for refinement we look for a tuple $\left(\mathcal{A}_N, (j_K)_{K \in \mathcal{A}_N}\right)$ as proposed in Section 3.2.2.

(S3) Refine the cells contained in $\mathcal{A}_N$ according to the refinement patterns $(j_K)_{K \in \mathcal{A}_N}$ and set $N := N+1$.
Continue with step (S1).

3.3. A Posteriori Error Estimate

An *a posteriori error estimate* is an upper bound of some error quantity, which only relies on information obtained from the solution of the discrete problem. Here we consider the energy error $\|\nabla(u - u_N)\|_{L^2(\Omega)}$ and prove

$$\|\nabla(u - u_N)\|_{L^2(\Omega)}^2 \leq \sum_{K \in \mathcal{K}_N} \varepsilon_K^2,$$

where the ε_K are some computable quantities that are local in K.

Theorem 1 (A posteriori error estimates)**.** *Let $\varepsilon > 0$ and $\mathcal{K}_N$ be a γ-shape regular mesh. Assume that for all $K_1, K_2 \in \mathcal{K}_N$ with $K_1 \cap K_2 \neq \emptyset$ holds*

$$\frac{p_{K_1}}{\gamma} \leq p_{K_2} \leq \gamma p_{K_1}. \tag{7}$$

Then there exists some constant $C_1 > 0$, independent of cell diameter h_K and polynomial degree p_K for all $K \in \mathcal{K}_N$, such that

$$\|\nabla(u - u_N)\|_{L^2(\Omega)}^2 \leq C_1 \sum_{K \in \mathcal{K}_N} \left(\eta_K^2 + \frac{h_K^2}{p_K^2} \|f - f_{p_K - 1}\|_{L^2(K)}^2 \right)$$

with η_K as in Definition 2. Further there exists some $C_2(\epsilon) > 0$, independent of h_K and p_K, such that

$$\eta_K^2 \leq C_2(\epsilon) \left(p_K^{2(1+\epsilon)} \|\nabla(u - u_N)\|_{L^2(\omega_K)}^2 + \frac{h_K^2}{p_K^{1-4\epsilon}} \|f_{p_K - 1} - f\|_{L^2(\omega_K)}^2 \right).$$

Proof. See [16], Lemmas 3.1, 3.4 and 3.5 with $\alpha = 0$. □

3.4. Convergence of hp-Adaptive Strategy

Now we will show the convergence of our refinement strategy in two space-dimensions. For this we have to show that the energy error decays in every refinement step, i. e. for $N \in \mathbb{N}_0$ and some $\kappa \in (0, 1)$ we have

$$\|\nabla(u - u_{N+1})\|_{L^2(\Omega)} \leq \kappa \|\nabla(u - u_N)\|_{L^2(\Omega)}.$$

Before we give the proof we first introduce an hp-efficient Scott–Zhang type interpolation operator, which was developed in [16] and is used in our proof later on. This interpolation operator is a generalization of the interpolation operator of [20] to the hp-context.
The following theorem states an upper bound for the interpolation error.

Theorem 2 (Scott–Zhang type interpolation)**.** *Let $\mathcal{K}$ be a γ-shape regular triangulation of Ω. Assume that assumption (7) holds for all $K_1, K_2 \in \mathcal{K}$ with $K_1 \cap K_2 \neq \emptyset$. Then there exist a linear operator $I : H_0^1(\Omega) \to S_0^p(\mathcal{K}, \Omega)$ and a constant $C_I > 0$, depending only on γ, such that*

1. *$Iu|_{\partial\Omega} = u|_{\partial\Omega} = 0$*
2. *For all $K \in \mathcal{K}$ holds*
$$\|u - Iu\|_{L^2(\omega_K)} \leq C_I \frac{h_K}{p_K} \|\nabla u\|_{L^2(\omega_{K,5})}.$$

Proof. In the vertex-based formulation (and notation) of Theorem 2.2 in [16] we have the two inequalities

$$\|u - Iu\|_{L^2(\omega_K)} \leq \sum_{V \in \mathcal{V}_K} \|u - Iu\|_{L^2(\omega_{V,1})}$$

and

$$\frac{h_V}{p_V} \|\nabla u\|_{L^2(\omega_{V,4})} \leq \frac{h_V}{p_V} \|\nabla u\|_{L^2(\omega_{K,5})} \leq C \frac{h_K}{p_K} \|\nabla u\|_{L^2(\omega_{K,5})},$$

where C depends solely on γ. Thus the result is a direct consequence of the cited theorem. □

Now we are ready to prove the convergence of our algorithm. This theorem is a generalization of Theorem 4 of [8] to two space-dimensions. The proof for the three-dimensional case follows the same arguments, but with three-dimensional versions of Theorems 1 and 2. For an idea on their proofs see [15].

Theorem 3 (Convergence)**.** *Let $N \in \mathbb{N}$ be arbitrary and $S_0^p(\mathcal{K}_N, \Omega)$ be the finite element space over a γ-shape regular discretization $\mathcal{K}_N$ of a bounded domain $\Omega \subset \mathbb{R}^2$. Further we assume that inequality (7) holds for all $K_1, K_2 \in \mathcal{K}_N$ with $K_1 \cap K_2 \neq \emptyset$. Let $u \in H_0^1(\Omega)$ be the solution of problem (2) and $u_N \in S_0^p(\mathcal{K}_N, \Omega)$ be the solution of the discrete problem (3) in iteration step N. Let $\theta \in [0, \min\{1, 2\sqrt{C_1}\}]$ and $\varepsilon > 1/2$ such that*

$$\theta^2 \geq \frac{8 C_1 C_{\mathrm{cov}} C^2}{\max\limits_{K \in \mathcal{K}_N} (p_K^{2\varepsilon})} \tag{8}$$

with C_1 from Theorem 1, C_{cov} from (12) and $C > 0$ depending only on γ. Further we assume that the data error is controlled by the discretization error, i.e. there exists some

$$\mu \in \left(0, \min\left\{1, \frac{1}{\sqrt{2C_2(\varepsilon) C_{\mathrm{cov}}} \max\limits_{K \in \mathcal{K}_N} \left(p_K^{2\varepsilon + \frac{1}{2}}\right)}\right\}\right)$$

independent of h_K, p_K, $K \in \mathcal{K}_N$, where $C_2(\varepsilon)$ is from Theorem 2, such that

$$\sum_{K \in \mathcal{K}_N} \frac{h_K^2}{p_K^2} \|f - f_{p_K - 1}\|_{L^2(K)}^2 \leq \mu^2 \sum_{K \in \mathcal{K}_N} \eta_K^2. \tag{9}$$

In addition we assume that in every refinement step $N \in \mathbb{N}$ the minimization problem (5), (6) has a solution $(\mathcal{A}_N, (j_K)_{K \in \mathcal{A}_N})$. Let $u_{N+1} \in S_0^p(\mathcal{K}_{N+1}, \Omega)$ be the solution of the discrete problem (3) in the following iteration step $N + 1$. Then there exists a constant $\kappa \in (0, 1)$ such that

$$\|\nabla(u - u_{N+1})\|_{L^2(\Omega)} \leq \kappa \|\nabla(u - u_N)\|_{L^2(\Omega)}.$$

Thus, if we run the hp-adaptive algorithm presented in Section 3.2.3, the energy error decreases uniformly in every iteration step.

Proof. Since $S_0^p(\mathcal{K}_N,\Omega)\subseteq S_0^p(\mathcal{K}_{N+1},\Omega)$, we can use the Galerkin orthogonality

$$\int_\Omega (\nabla(u-u_{N+1}))^T\nabla(u_{N+1}-u_N)=0$$

to get

$$\|\nabla(u-u_N)\|^2_{L^2(\Omega)}=\|\nabla(u-u_{N+1})\|^2_{L^2(\Omega)}+\|\nabla(u_{N+1}-u_N)\|^2_{L^2(\Omega)}.$$

Thus the proof follows, if there exists some $\kappa\in(0,1)$ such that

$$\|\nabla(u_{N+1}-u_N)\|^2_{L^2(\Omega)}\geq(1-\kappa^2)\|\nabla(u-u_N)\|^2_{L^2(\Omega)}. \tag{10}$$

Let $K\in\mathcal{K}_N$ and $v_{N+1}\in S_0^p(\mathcal{K}_{N+1},\Omega)$ with $\operatorname{supp}(v_{N+1})\subset\omega_K$. Then by Galerkin orthogonality we see

$$\begin{aligned}\int_{\omega_K}(\nabla v_{N+1})^T\nabla(u_{N+1}-u_N)&=\int_{\omega_K}(\nabla v_{N+1})^T\nabla(u_{N+1}-u+u-u_N)\\&=\int_{\omega_K}(v_{N+1}f-(\nabla v_{N+1})^T\nabla u_N)\\&=\int_{\omega_K}(v_{N+1}f_{p_{\omega_K}}-(\nabla v_{N+1})^T\nabla u_N)+\int_{\omega_K}v_{N+1}\left(f-f_{p_{\omega_K}}\right).\end{aligned}$$

Using the definition of $f_{p_{\omega_K}}$ we get

$$\begin{aligned}&\int_{\omega_K}(\nabla v_{N+1})^T\nabla(u_{N+1}-u_N)\\&\qquad=\int_{\omega_K}(v_{N+1}f_{p_{\omega_K}}-(\nabla v_{N+1})^T\nabla u_N)+\int_{\omega_K}(v_{N+1}-v_N)\left(f-f_{p_{\omega_K}}\right),\end{aligned}$$

which implies

$$\begin{aligned}&\left|\int_{\omega_K}(\nabla v_{N+1})^T\nabla(u_{N+1}-u_N)\right|\\&\qquad\geq\left|\int_{\omega_K}(v_{N+1}f_{p_{\omega_K}}-(\nabla v_{N+1})^T\nabla u_N)\right|-\left|\int_{\omega_K}(v_{N+1}-v_N)\left(f-f_{p_{\omega_K}}\right)\right|,\end{aligned}$$

and applying the Cauchy–Schwarz inequality yields

$$\begin{aligned}&\left|\int_{\omega_K}(v_{N+1}f_{p_{\omega_K}}-(\nabla v_{N+1})^T\nabla u_N)\right|\\&\qquad\leq\|\nabla v_{N+1}\|_{L^2(\omega_K)}\|\nabla(u_{N+1}-u_N)\|_{L^2(\omega_K)}+\|v_{N+1}-v_N\|_{L^2(\omega_K)}\left\|f-f_{p_{\omega_K}}\right\|_{L^2(\omega_K)}.\end{aligned}\tag{11}$$

Choosing $v_N:=I_Nv_{N+1}$ with $I_N:H_0^1(\Omega)\to S_0^p(\mathcal{K}_N,\Omega)$ as in Theorem 2 implies

$$\|v_{N+1}-v_N\|_{L^2(\omega_K)}=\|v_{N+1}-I_Nv_{N+1}\|_{L^2(\omega_K)}\leq C_I\frac{h_K}{p_K}\|\nabla v_{N+1}\|_{L^2(\omega_{K,5})}.$$

Since $\operatorname{supp}(v_{N+1})\subset\omega_K\subset\omega_{K,5}$ we have

$$\|v_{N+1}-v_N\|_{L^2(\omega_K)}\leq C_I\frac{h_K}{p_K}\|\nabla v_{N+1}\|_{L^2(\omega_K)}$$

and inserting into (11) yields

$$\left|\int_{\omega_K}(v_{N+1}f_{p_{\omega_K}}-(\nabla v_{N+1})^T\nabla u_N)\right| \\ \leq \left(\|\nabla(u_{N+1}-u_N)\|_{L^2(\omega_K)}+C_I\frac{h_K}{p_K}\left\|f-f_{p_{\omega_K}}\right\|_{L^2(\omega_K)}\right)\|\nabla v_{N+1}\|_{L^2(\omega_K)}.$$

Dividing by $\|\nabla v_{N+1}\|_{L^2(\omega_K)}$ and taking the supremum on both sides yields

$$\sup_{\phi\in S^p_{0,K,j_K}(\mathcal{K}_N,\omega_K)}\left(\frac{\int_{\omega_K}(\phi f_{p_{\omega_K}}-(\nabla\phi)^T\nabla u_N)}{\|\nabla\phi\|_{L^2(\omega_K)}}\right) \\ \leq \sup_{\substack{v_{N+1}\in S^p_0(\mathcal{K}_{N+1},\Omega)\\ \operatorname{supp}(v_{N+1})\subset\omega_K}}\left(\frac{\int_{\omega_K}(v_{N+1}f_{p_{\omega_K}}-(\nabla v_{N+1})^T\nabla u_N)}{\|\nabla v_{N+1}\|_{L^2(\omega_K)}}\right) \\ \leq \|\nabla(u_{N+1}-u_N)\|_{L^2(\omega_K)}+C_I\frac{h_K}{p_K}\left\|f-f_{p_{\omega_K}}\right\|_{L^2(\omega_K)}$$

and with (4) we have

$$\beta_{K,j_K}\eta_K\leq\|\nabla(u_{N+1}-u_N)\|_{L^2(\omega_K)}+C_I\frac{h_K}{p_K}\left\|f-f_{p_{\omega_K}}\right\|_{L^2(\omega_K)}.$$

Squaring both sides and summing up over $K\in\mathcal{K}_N$ yields

$$\sum_{K\in\mathcal{A}_N}(\beta_{K,j_K}\eta_K)^2\leq\sum_{K\in\mathcal{K}_N}(\beta_{K,j_K}\eta_K)^2 \\ \leq 2\left(\sum_{K\in\mathcal{K}_N}\|\nabla(u_{N+1}-u_N)\|^2_{L^2(\omega_K)}+C_I^2\sum_{K\in\mathcal{K}_N}\frac{h_K^2}{p_K^2}\left\|f-f_{p_{\omega_K}}\right\|^2_{L^2(\omega_K)}\right) \\ \leq 2C_{\mathrm{cov}}\left(\|\nabla(u_{N+1}-u_N)\|^2_{L^2(\Omega)}+C^2\sum_{K\in\mathcal{K}_N}\frac{h_K^2}{p_K^2}\|f-f_{p_K-1}\|^2_{L^2(K)}\right)$$

(use the minimal property of $f_{p_{\omega_K}}$ in $L^2(\omega_K)$) with the covering constant

$$C_{\mathrm{cov}}:=\max_{K\in\mathcal{K}_N}|\{L\in\mathcal{K}_N:L\subset\omega_K\}|, \tag{12}$$

where $|A|$ denotes the cardinality of the set A, and $C>0$ is a constant that depends only on γ. Finally by assumption (9) we get

$$\sum_{K\in\mathcal{A}_N}(\beta_{K,j_K}\eta_K)^2\leq 2C_{\mathrm{cov}}\left(\|\nabla(u_{N+1}-u_N)\|^2_{L^2(\Omega)}+C^2\mu^2\sum_{K\in\mathcal{K}_N}\eta_K^2\right). \tag{13}$$

From Theorem 1 we know that there exists some $C_1>0$ such that

$$\|\nabla(u-u_N)\|^2_{L^2(\Omega)}\leq C_1\sum_{K\in\mathcal{K}_N}\left(\eta_K^2+\frac{h_K^2}{p_K^2}\|f-f_{p_K-1}\|^2_{L^2(K)}\right) \\ \leq C_1(1+\mu^2)\sum_{K\in\mathcal{K}_N}\eta_K^2 \\ \leq 2C_1\sum_{K\in\mathcal{K}_N}\eta_K^2$$

by (9) (and $\mu \leq 1$). Multiplying both sides by $\theta^2 \in [0,1]$ yields

$$\theta^2 \|\nabla(u-u_N)\|^2_{L^2(\Omega)} \leq 2C_1\theta^2 \sum_{K\in\mathcal{K}_N} \eta_K^2$$

and by applying inequality (6) with $\varepsilon_K := \eta_K$ we have

$$\theta^2 \|\nabla(u-u_N)\|^2_{L^2(\Omega)} \leq 2C_1 \sum_{K\in\mathcal{A}_N} \left(\beta_{K,j_K}\eta_K\right)^2.$$

Then we see

$$\theta^2 \|\nabla(u-u_N)\|^2_{L^2(\Omega)} \leq 4C_1C_{\text{cov}} \left(\|\nabla(u_{N+1}-u_N)\|^2_{L^2(\Omega)} + C^2\mu^2 \sum_{K\in\mathcal{K}_N} \eta_K^2 \right) \tag{14}$$

by equation (13). From Theorem 1 we know

$$\begin{aligned}
\sum_{K\in\mathcal{K}_N} \eta_K^2 &\leq C_2(\varepsilon) \sum_{K\in\mathcal{K}_N} \left(p_K^{2(\varepsilon+1)} \|\nabla(u-u_N)\|^2_{L^2(\omega_K)} + \frac{h_K^2}{p_K^{1-4\varepsilon}} \|f-f_{p_K-1}\|^2_{L^2(\omega_K)} \right) \\
&\leq C_2(\varepsilon)C_{\text{cov}} \left(\max_{K\in\mathcal{K}_N} \left(p_K^{2(\varepsilon+1)}\right) \|\nabla(u-u_N)\|^2_{L^2(\Omega)} + \max_{K\in\mathcal{K}_N} \left(p_K^{4\varepsilon+1}\right) \sum_{K\in\mathcal{K}_N} \frac{h_K^2}{p_K^2} \|f-f_{p_K-1}\|^2_{L^2(K)} \right)
\end{aligned}$$

and assumption (9) yields

$$\sum_{K\in\mathcal{K}_N} \eta_K^2 \leq C_2(\varepsilon)C_{\text{cov}} \left(\max_{K\in\mathcal{K}_N} \left(p_K^{2(\varepsilon+1)}\right) \|\nabla(u-u_N)\|^2_{L^2(\Omega)} + \mu^2 \max_{K\in\mathcal{K}_N} \left(p_K^{4\varepsilon+1}\right) \sum_{K\in\mathcal{K}_N} \eta_K^2 \right).$$

Hence for

$$\mu < \frac{1}{\sqrt{C_2(\varepsilon)C_{\text{cov}}} \max\limits_{K\in\mathcal{K}_N} \left(p_K^{2\varepsilon+\frac{1}{2}}\right)}$$

we have

$$\sum_{K\in\mathcal{K}_N} \eta_K^2 \leq \frac{C_2(\varepsilon)C_{\text{cov}} \max\limits_{K\in\mathcal{K}_N} \left(p_K^{2(\varepsilon+1)}\right)}{1-\mu^2 C_2(\varepsilon)C_{\text{cov}} \max\limits_{K\in\mathcal{K}_N} \left(p_K^{4\varepsilon+1}\right)} \|\nabla(u-u_N)\|^2_{L^2(\Omega)}$$

and with the even more restrictive assumption

$$\mu < \frac{1}{\sqrt{2C_2(\varepsilon)C_{\text{cov}}} \max\limits_{K\in\mathcal{K}_N} \left(p_K^{2\varepsilon+\frac{1}{2}}\right)} \tag{15}$$

we get

$$\sum_{K\in\mathcal{K}_N} \eta_K^2 \leq 2C_2(\varepsilon)C_{\text{cov}} \max_{K\in\mathcal{K}_N} \left(p_K^{2(\varepsilon+1)}\right) \|\nabla(u-u_N)\|^2_{L^2(\Omega)}.$$

Inserting into (14) yields

$$\begin{aligned}
&\theta^2 \|\nabla(u-u_N)\|^2_{L^2(\Omega)} \\
&\quad \leq 4C_1C_{\text{cov}} \left(\|\nabla(u_{N+1}-u_N)\|^2_{L^2(\Omega)} + 2\mu^2 C_2(\varepsilon)C_{\text{cov}}C^2 \max_{K\in\mathcal{K}_N} \left(p_K^{2(\varepsilon+1)}\right) \|\nabla(u-u_N)\|^2_{L^2(\Omega)} \right)
\end{aligned}$$

and by (15) we get

$$\theta^2\|\nabla(u-u_N)\|^2_{L^2(\Omega)} \leq 4C_1C_{\mathrm{cov}}\left(\|\nabla(u_{N+1}-u_N)\|^2_{L^2(\Omega)} + \frac{C^2}{\max\limits_{K\in\mathcal{K}_N}(p_K^{2\varepsilon-1})}\|\nabla(u-u_N)\|^2_{L^2(\Omega)}\right).$$

Therefore

$$\frac{1}{4C_1C_{\mathrm{cov}}}\left(\theta^2 - \frac{4C_1C_{\mathrm{cov}}C^2}{\max\limits_{K\in\mathcal{K}_N}(p_K^{2\varepsilon-1})}\right)\|\nabla(u-u_N)\|^2_{L^2(\Omega)} \leq \|\nabla(u_{N+1}-u_N)\|^2_{L^2(\Omega)}$$

and by (8) we have

$$\theta^2 - \frac{4C_1C_{\mathrm{cov}}C^2}{\max\limits_{K\in\mathcal{K}_N}(p_K^{2\varepsilon-1})} \geq \frac{1}{2}\theta^2.$$

Since $C_{\mathrm{cov}} > 1$ and $\theta < 2\sqrt{C_1}$, inequality (10) holds with

$$\kappa^2 := 1 - \frac{\theta^2}{4C_1C_{\mathrm{cov}}}.$$

This completes the proof of the theorem. □

Remark 2.

1. *For $\theta \in [0, \min\{1, 2\sqrt{C_1}\}]$ assumption* (8) *can always be satisfied by choosing p_K big enough for some $K \in \mathcal{K}_N$. However, the qualitative convergence result might be a first step towards proving optimality [5, 21].*
2. *The data saturation assumption* (9) *can only be satisfied, if the integrals on the left-hand side are computed with negligible error. To achieve this one can use high-order quadrature rules and perform local refinement according to the local error indicator*

$$\frac{h_K^2}{p_K^2}\|f - f_{p_K-1}\|^2_{L^2(K)}$$

   until (9) *is satisfied or build some data error control into the whole algorithm as proposed in [14, 17].*
3. *If the computed values β_{K,j_K} are too small or θ is chosen too large, then the solution $(\mathcal{A}_N, (j_K)_{K\in\mathcal{A}_N})$ of the minimization problem* (5), (6) *might not exist for some $N \in \mathbb{N}$. Especially this is the case if*

$$\max_{K\in\mathcal{A}_N}\beta_{K,j_K} < \theta.$$

   Then our algorithm will continue with global refinement, but a uniform decrease of the error cannot be guaranteed anymore.
4. *If β_{K,j_K} is uniformly bounded from below, then there is a choice for θ such that convergence according to Theorem 3 is assured. We think this can be shown following the ideas in [8], Theorem 5. However, this property can also be assured by monitoring the known values of β_{K,j_K} thus checking the convergence in an a posteriori way.*

4. Numerical Results

We apply our refinement strategy to some representative problems of the form (1). For both, two and three space-dimensions, we choose one example with a smooth solution and one with a singular solution to show how the refinement strategy behaves under these very different circumstances. The computations are performed with the finite element library deal.II [3, 4] in combination with parts of the *Trilinos Project* [10, 11].

4.1. Example 1

In the first example our algorithm is applied to a problem of the form (1) with a smooth solution. Let $\Omega := (0,1)^2$, $g := 0$ and

$$u(x,y) := x(1-x)y(1-y)(1-2y)\exp\left(-2.5(2x-1)^2\right).$$

We start our algorithm with the triangulation $\mathcal{K}_0$ consisting of 64 cells of same size. As refinement patterns we offer the usual bisection in every coordinate-direction of a cell as h-refinement and the increment of the polynomial degree of the cell by one as p-refinement. We denote this strategy by Θ_1. As initial polynomial degree we choose $p = 2$ on all cells. For $\theta \in [0,1]$ we choose $\theta := 0.35$. In Figure 3 we plot the number of degrees of freedom vs. the true energy error respectively the estimated error in $\log_{10}$-$\log_{10}$-scale on the left-hand side and the distribution of the polynomial degree on the final grid on the right-hand side. In Table 1 on the left-hand side the marking history is shown. There we denote the number of cells marked for h-refinement by $\#h$ and the number of cells marked for p-refinement by $\#p$. We observe that no h-refinement takes place and the algorithm performs full p-refinement in every refinement step, which is the case because the solution u is very smooth. On the final grid the polynomial degree is equally distributed with value 8. In Figure 4 we plot θ vs. the number of degrees of freedom on the left-hand side and θ vs. the number of refinement steps on the right-hand side. There we can see that the minimal number of degrees of freedom we achieved is 1967, which is attained for $\theta = 0.1$. For $\theta \geq 0.35$ global refinement is performed. The number of refinement steps decays for increasing θ. In Figure 5 on the left-hand side we plot θ vs. the computation time in seconds. The minimal computation time we achieved is approx. 1.91 s. This supports our choice $\theta = 0.35$. For $K \in \mathcal{K}_0$ we have $\beta_{K,j_K} \in [0.27, 0.58]$. Thus the optimal value for θ lies near the minimal value of β_{K,j_K}.

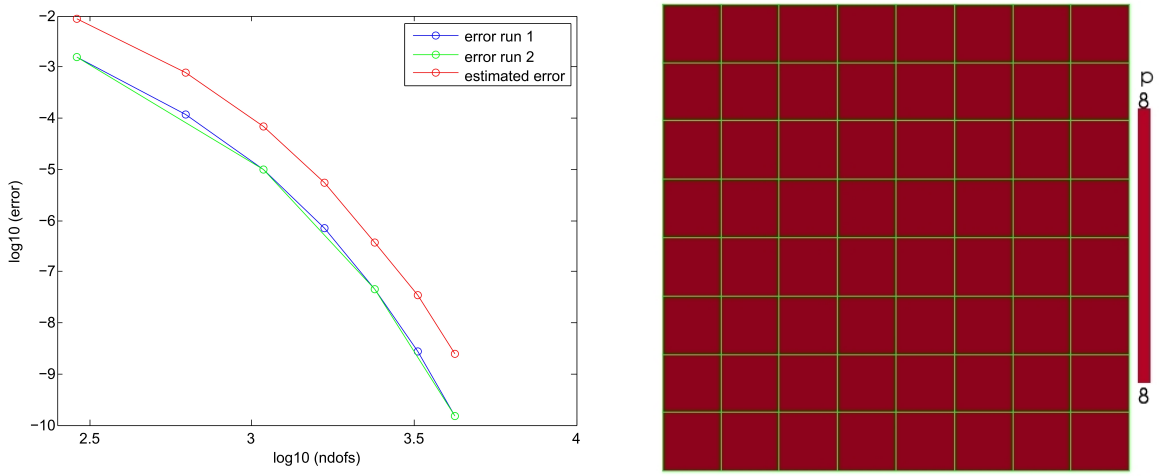

Figure 3: Example 1: Strategy Θ_1. Left: Number of degrees of freedom vs. error. Right: Distribution of polynomial degree.

In a second try we add the increment of the polynomial degree by two as a third refinement possibility to the algorithm. We denote this refinement strategy by Θ_2. In Figure 3 on the left-hand side we plot the number of degrees of freedom vs. the true energy error respectively the estimated error in $\log_{10}$-$\log_{10}$-scale. We note that this strategy produces the same final result as Θ_1, but with half the number of refinement steps. In Figure 4 we plot θ vs. the number of degrees of freedom and θ vs. the number of refinement steps. The minimal number of degrees of freedom we achieved for this run is 2401 for $\theta = 0.35$. The number of refinement steps is reduced significantly with this third refinement pattern in use and the computation time is reduced to approx. 1.26 s.

Step	#Cells	max(p)	$\#h$	$\#p$
0	64	2	0	64
1	64	3	0	64
2	64	4	0	64
3	64	5	0	64
4	64	5	0	64
5	64	6	0	64
6	64	7	0	64

Step	#Cells	max(p)	$\#h$	$\#p$
0	64	2	0	8
1	64	3	0	24
2	64	4	0	24
3	64	5	0	24
4	64	6	0	24
5	64	7	9	24

Table 1: Left: Example 1. Marking history. Right: Example 3. Marking history.

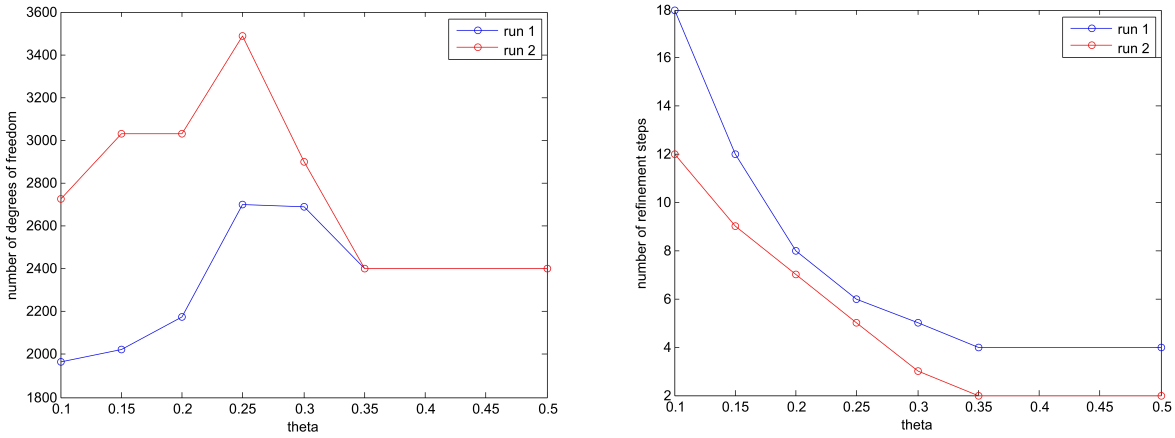

Figure 4: Example 1. Left: θ vs. number of degrees of freedom. Right: θ vs. number of refinement steps.

4.2. Example 2

The second example shows how the algorithm performs, if the solution of model problem (1) has a corner singularity.

Let $\Omega := (-1,1)^2 \setminus [0,1) \times (-1,0]$, $f := 0$ and

$$u(r,\phi) := r^{\frac{2}{3}} \sin\left(\frac{2}{3}\phi\right),$$

where $r \in [0,1)$ and $\phi \in [0,2\pi)$ denote the polar coordinates, and $g := u$. Again we use refinement strategy Θ_1. We start our computations with initial grid $\mathcal{K}_0$ consisting of 48 cells of the same size and polynomial degree $p = 2$ on every cell. We choose $\theta = 0.25$. In Figure 5, on the right-hand side, we plot the number of degrees of freedom vs. the true energy error respectively the estimated error in $\log_{10}$-$\log_{10}$-scale. The distribution of the polynomial degree on the final grid is shown in Figure 6 on the left-hand side. We see that the algorithm performs h-refinement around the singularity located at 0 only. The polynomial degree is raised up to 8 away from the singularity. In Table 2 the marking history is shown. We observe that the algorithm starts with some h-refinements around the singularity and then performs more and more p-refinements. In Figure 6 we plot θ vs. the number of degrees of freedom on the right-hand side. There we can see that the number of degrees of freedom increases for increasing θ until $\theta = 0.3$. For $\theta \geq 0.3$ the number of degrees of freedom stays constant at its maximum value 14457, since in this range global refinement is performed. The minimal number of degrees of freedom we achieved is 2690 for $\theta = 0.15$. θ vs. the number of refinement steps is shown in Figure 7 on the left-hand side. We observe that the number of refinement steps decays for increasing θ. Further we see that the number of

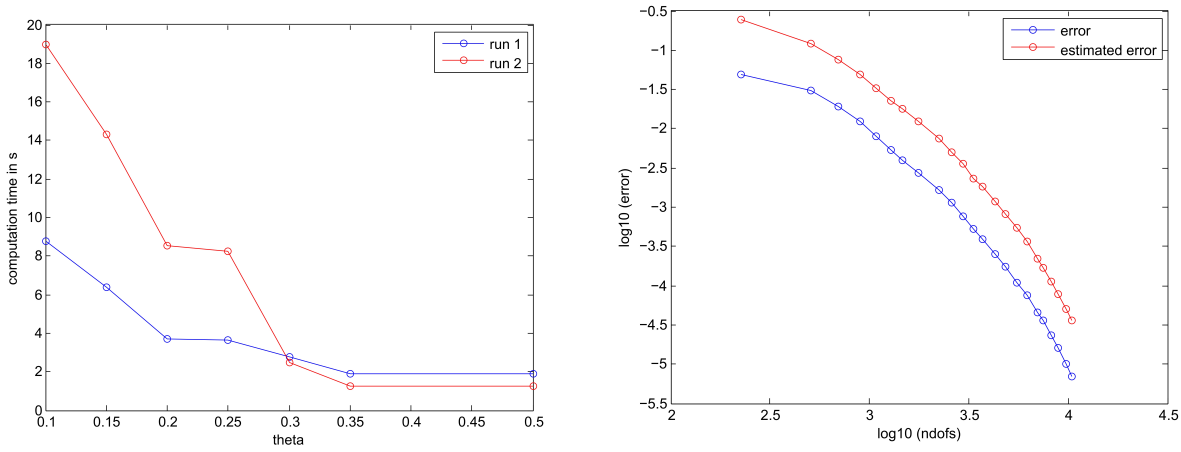

Figure 5: Left: Example 1. θ vs. computation time. Right: Strategy Θ_2. Number of degrees of freedom vs. error.

degrees of freedoms and the number of refinement steps change 'discontinuously' in the interval $[0.25, 0.3]$. This behaviour can also be observed in the computation time, which is required for the different values of θ – see Figure 7 on the right-hand side. The minimal computation time is achieved for $\theta = 0.25$ and we see that with $\beta_{K,j_K} \in [0.18, 1]$ for $K \in \mathcal{K}_0$ we have a good indicator for the choice of θ again.

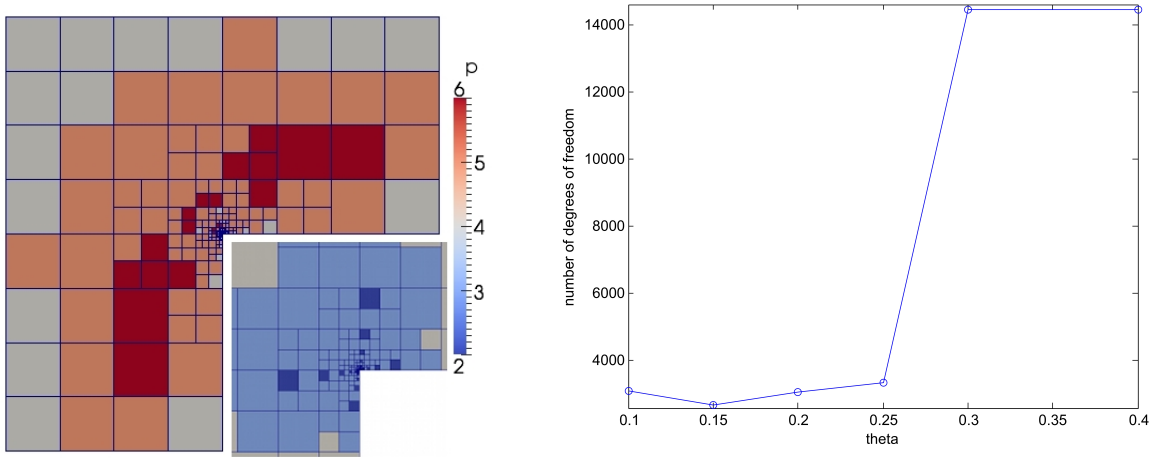

Figure 6: Example 2. Left: Distribution of polynomial degree. Right: θ vs. number of degrees of freedom.

4.3. Example 3

Now we investigate the performance of our hp-adaptive refinement strategy in three space-dimensions. First we consider a smooth example again. Let $\Omega := [0,1]^3$, $u(x,y,z) := \sin(\pi x)\sin(\pi y)\sin(\pi z)$, $f := 3\pi^2 u$ and $g := 0$. We use refinement strategy Θ_1 and start our computations with initial grid $\mathcal{K}_0$ consisting of 64 equally sized cells. As initial polynomial degree we choose $p = 2$ on all cells. We choose $\theta = 0.2$. In Figure 8 we plot the number of degrees of freedom vs. the true energy error respectively the estimated error in $\log_{10}$-$\log_{10}$-scale on the left-hand side. We can see that the polynomial degree equals 8 on all cells except the ones located at the corners. There the polynomial degree is raised to 7 only. In Table 1 on the right-hand side the marking history is shown. We observe that the algorithm performs p-refinements

Step	#Cells	max(p)	h	p	Step	#Cells	max(p)	h	p
0	48	2	3	2	11	345	4	3	10
1	75	3	3	0	12	372	4	3	18
2	102	3	3	0	13	399	4	3	18
3	129	3	3	0	14	426	4	3	22
4	156	3	3	0	15	453	5	3	23
5	183	3	3	0	16	480	5	3	28
6	210	3	3	4	17	507	6	3	12
7	237	3	3	10	18	534	6	3	22
8	264	4	3	10	19	561	6	1	28
9	291	4	3	11	20	576	6	1	32
10	318	4	3	10	21	591	6	1	26

Table 2: Example 2. Marking history

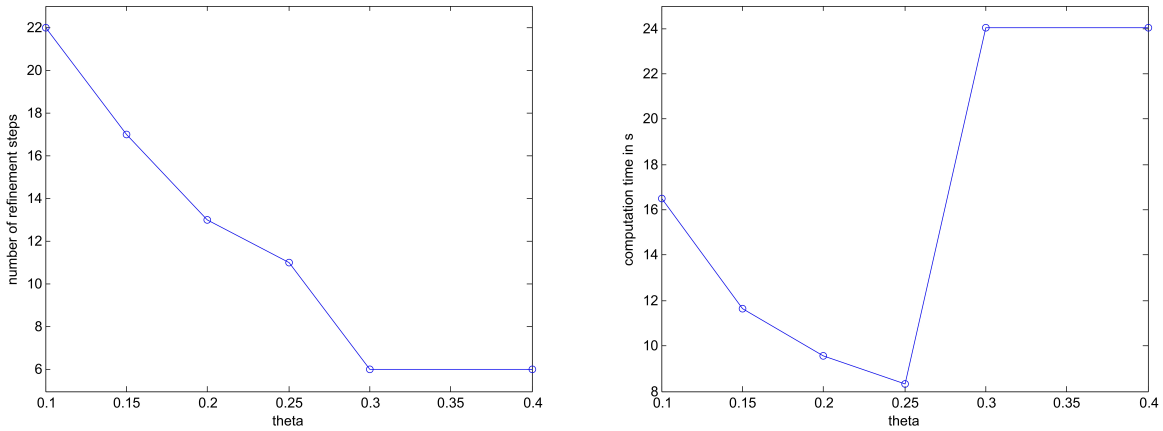

Figure 7: Example 2. Left: θ vs. number of refinement steps. Right: θ vs. computation time.

only. In Figure 9 we plot θ vs. the number of degrees of freedom on the left-hand side. There we can see that the number of degrees of freedom stays constant unless a jump at $\theta = 0.235$. This is due to the point-wise symmetry of the analytic solution. For $\theta \leq 0.23$ the number of degrees of freedom is 24333 and for $\theta \geq 0.24$ the number of degrees of freedom is 24389. The number of refinement steps has constant value 5 for all $\theta \in [0, 1]$. In Figure 7 on the right-hand side we plot θ vs. the computation time in seconds. For $K \in \mathcal{K}_0$ we have $\beta_{K,j_K} \in [0.27, 0.63]$. Hence the optimal value for θ lies again near the minimal value of β_{K,j_K}.

In a second try we use the refinement strategy Θ_2. We plot the number of degrees of freedom vs. the true error in Figure 10 on the left-hand side. The distribution of the polynomial degree is shown on the right-hand side. We observe that also strategy Θ_2 raises the polynomial degree to 8 on all cells except the ones located at the corners. There the polynomial degree has value 6 only.

4.4. Example 4

In our last example we consider again a problem with a corner singularity. Let $\Omega := [-1, 1]^3 \setminus (0, 1]^3$,

$$u(x, y, z) := \left(x^2 + y^2 + z^2\right)^{\frac{1}{3}}, \quad f(x, y, z) := -\frac{10}{9\left(x^2 + y^2 + z^2\right)^{\frac{2}{3}}}$$

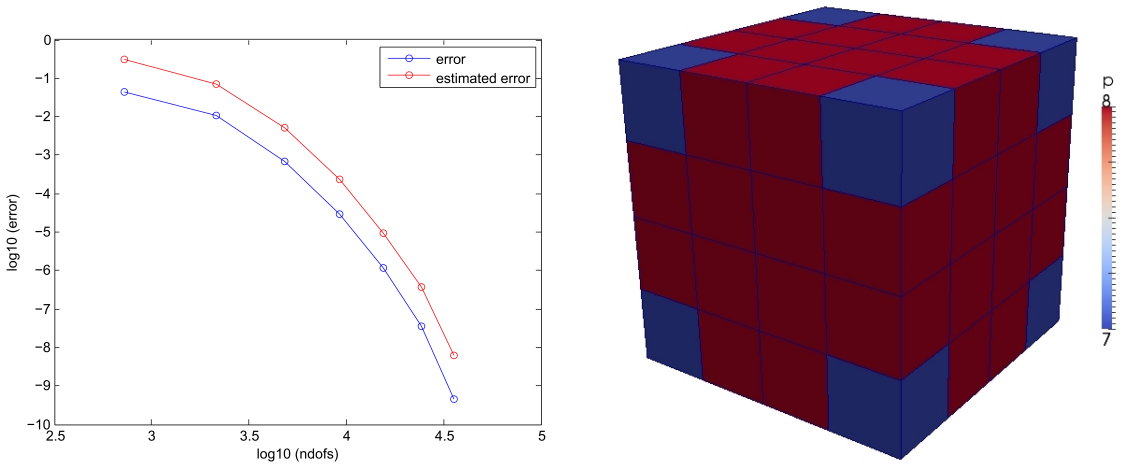

Figure 8: Example 3: Θ_1. Left: Number of degrees of freedom vs. error. Right: Distribution of polynomial degree.

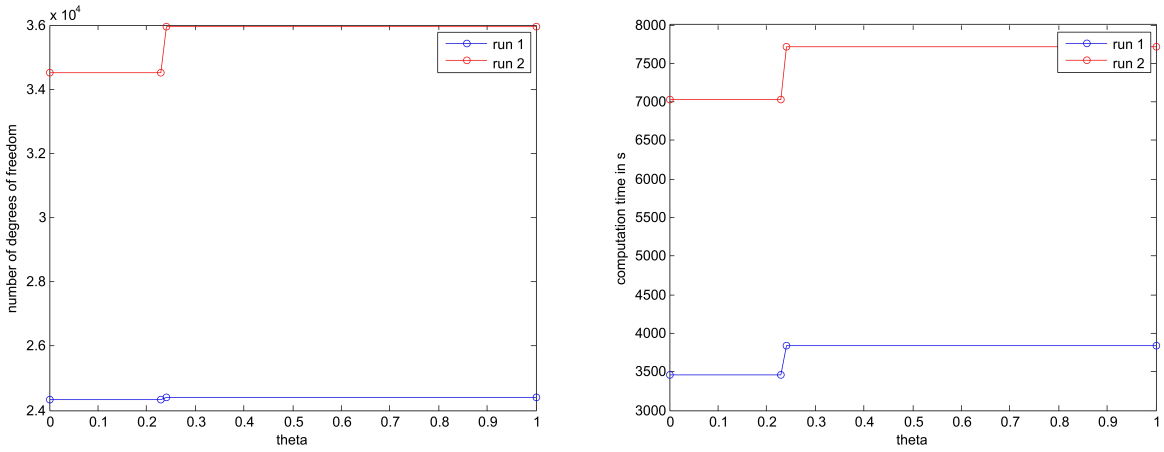

Figure 9: Example 3. Left: θ vs. number of degrees of freedom. Right: θ vs. computing time.

and $g := u$. Again we use refinement strategy Θ_1 and start our computations with initial grid $\mathcal{K}_0$ consisting of 448 equally sized cells and polynomial degree $p = 2$ on all cells. We choose $\theta = 0.16$. In Figure 11 on the left-hand side we plot the number of degrees of freedom vs. the true energy error respectively the estimated error in $\log_{10}$-$\log_{10}$-scale. In Table 3 we show the marking history. We observe that the algorithm starts with some h-refinements around the singularity located at 0 and then performs more and more p-refinements. In Figure 11 we plot θ vs. the number of degrees of freedom. There we can see that the number of degrees of freedom is increasing for $\theta \leq 0.21$. Then the number of degrees of freedom stays constant at 1349548. The minimal number of degrees of freedoms we achieved is 519342 for $\theta = 0.16$. For $\theta \geq 0.16$ the number of refinement steps is constant as can be seen in Figure 12. Only for $\theta = 0.16$ the algorithm requires more refinement steps. For $K \in \mathcal{K}_0$ we have $\beta_{K,j_K} \in [0.15, 1]$. Also in this example the minimal value of β_{K,j_K} is a good indicator for the choice of θ.

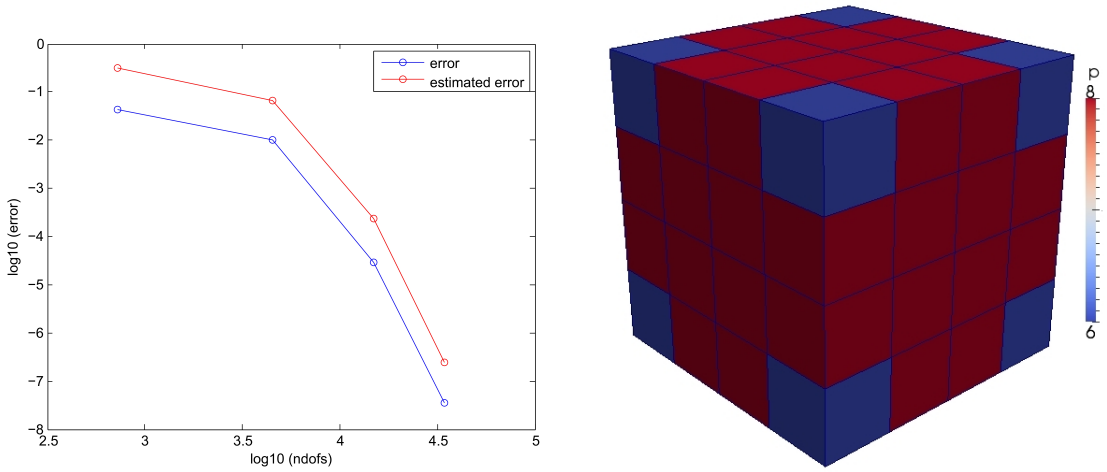

Figure 10: Example 3: Θ_2. Left: Number of degrees of freedom vs. error. Right: Distribution of polynomial degree.

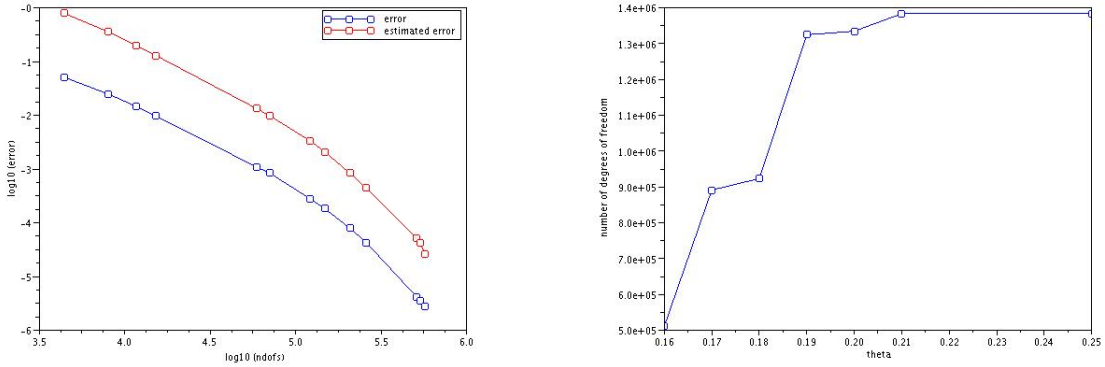

Figure 11: Example 4: Left: Number of degrees of freedom vs. error. Right: θ vs. number of degrees of freedom.

[1] M. Ainsworth and T.J. Oden. *A Posteriori Error Estimation in Finite Element Analysis*. Wiley, New York, 2000.

[2] M. Ainsworth and B. Senior. An adaptive refinement strategy for *hp*-finite element computations. *Appl. Numer. Math.*, 26:165–178, 1998.

[3] W. Bangerth, R. Hartmann, and G. Kanschat. `deal.II` *Differential Equations Analysis Library, Technical Reference*. `http://www.dealii.org`.

[4] W. Bangerth, R. Hartmann, and G. Kanschat. deal.II — a general-purpose object-oriented finite element library. *ACM Trans. Math. Softw.*, 33(4), 2007.

[5] P. Binev, W. Dahmen, and R. DeVore. Adaptive finite element methods with convergence rates. *Numer. Math.*, 97:219–268, 2004.

[6] L. Demkowicz, W. Rachowicz, and Ph. Devloo. A fully automatic *hp*-adaptivity. *J. Sci. Comp.*, 17(1–3):127–155, 2002.

Step	#Cells	max(p)	h	p	Step	#Cells	max(p)	h	p
0	448	2	7	0	6	2506	4	7	28
1	791	2	7	0	7	2849	4	7	182
2	1134	2	7	0	8	3192	5	7	77
3	1477	2	7	147	9	3535	5	7	352
4	1820	3	7	0	10	3876	6	6	0
5	2163	3	7	98	11	4200	6	7	7

Table 3: Example 4. Marking history.

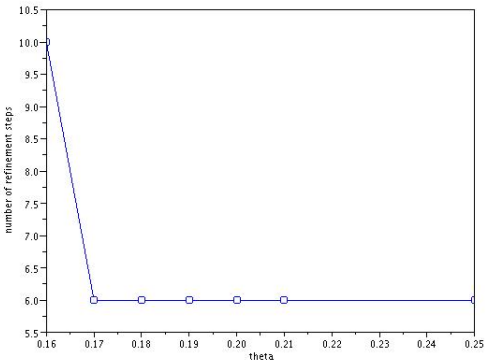

Figure 12: Example 4: θ vs. number of refinement steps.

[7] W. Dörfler. A convergent adaptive algorithm for Poisson's equation. *SIAM J. Numer. Anal.*, 33:1106–1124, 1996.

[8] W. Dörfler and V. Heuveline. Convergence of an adaptive *hp* finite element strategy in one space dimension. *Appl. Numer. Math.*, 57:1108–1124, 2007.

[9] T. Eibner and J.M. Melenk. An adaptive strategy for *hp*-FEM based on testing for analyticity. *Comput. Mech.*, 39:575–595, 2007.

[10] M. Heroux, R. Bartlett, V.H.R. Hoeckstra, J. Hu, T. Kolda, R. Lehoucq, K. Long, R. Pawlowski, E. Phipps, A. Salinger, H. Thornquist, R. Tuminaro, J. Willenbring, and A. Williams. An overview of Trilinos. Technical Report SAND2003-2927, Sandia National Labs, 2003.

[11] M. Heroux, R. Bartlett, V.E. Howle, R.J. Hoeckstra, J. Hu, T. Kolda, R. Lehoucq, K. Long, R. Pawlowski, E. Phipps, A. Salinger, H. Thornquist, R. Tuminaro, J. Willenbring, A. Williams, and K. Stanley. An overview of the Trilinos project. *ACM Trans. Math. Softw.*, 31(3):397–423, 2005.

[12] V. Heuveline and R. Rannacher. Duality-based adaptivity in the *hp*-finite element method. *J. Numer. Math.*, 11(2):95–113, 2003.

[13] P. Houston and E. Süli. A note on the design of *hp*-adaptive finite element methods for elliptic partial differential equations. *Comput. Meth. Appl. Mech. Eng.*, 194:229–243, 2005.

[14] K. Mekchay and R.H. Nochetto. Convergence of adaptive finite element methods for general second order ellliptic PDEs. *SIAM J. Numer. Anal.*, 43(5):1803–1827, 2005.

[15] J.M. Melenk. *hp*-interpolation of nonsmooth functions and an application to *hp*-a posteriori error estimation. *SIAM J. Numer. Anal.*, 43(1):127–155, 2005.

[16] J.M. Melenk and B.I. Wohlmuth. On residual-based a posteriori error estimation in *hp*-FEM. *Adv. Comp. Math.*, 15:311–331, 2001.

[17] P. Morin, R.H. Nochetto, and K.G. Siebert. Data oscillation and convergence of adaptive FEM. *SIAM J. Numer. Anal.*, 38:466–488, 2000.

[18] W. Rachowicz, D. Pardo, and L. Demkowicz. Fully automatic *hp*-adaptivity in three dimensions. *Comp. Meth. Appl. Mech. Eng.*, 195:4816–4842, 2006.

[19] Ch. Schwab. *p- and hp-Finite Element Methods*. Clarendon Press, Oxford, 1998.

[20] L.R. Scott and S. Zhang. Finite element interpolation of nonsmooth functions satisfying boundary conditions. *Math. Comp.*, 54:483–493, 1990.

[21] R. Stevenson. Optimality of a standard adaptive finite element method. *Found. Comput. Math.*, 7(2):245–269, 2007.

[22] B. Szabó and I. Babuška. *Finite Element Analysis*. Wiley, New York, 1991.

[23] R. Verfürth. *A review of* A Posteriori *Error Estimation and Adaptive Mesh-Refinement Techniques*. Wiley/Teubner, Chichester, 1996.

IWRMM-Preprints seit 2008

Nr. 08/01 Patrizio Neff, Antje Sydow, Christian Wieners: Numerical approximation of incremental infinitesimal gradient plasticity

Nr. 08/02 Götz Alefeld, Zhengyu Wang: Error Estimation for Nonlinear Complementarity Problems via Linear Systems with Interval Data

Nr. 08/03 Ulrich Kulisch : Complete Interval Arithmetic and its Implementation on the Computer

Nr. 08/04 Armin Lechleiter, Andreas Rieder: Newton Regularizations for Impedance Tomography: Convergence by Local Injectivity

Nr. 08/05 Vu Hoang, Michael Plum, Christian Wieners: A computer-assisted proof for photonic band gaps

Nr. 08/06 Vincent Heuveline, Peter Wittwer: Adaptive boundary conditions for exterior stationary flows in three dimensions

Nr. 08/07 Jan Mayer: Parallel Algorithms for Solving Linear Systems with Sparse Triangular Matrices

Nr. 08/08 Ulrich Kulisch : Begegnungen eines Mathematikers mit Informatik

Nr. 08/09 Tomas Dohnal, Michael Plum, Wolfgang Reichel: Localized Modes of the Linear Periodic Schrödinger Operator with a Nonlocal Perturbation

Nr. 08/10 Götz Alefeld: Verified Numerical Computation for Nonlinear Equations

Nr. 08/11 Götz Alefeld, Zhengyu Wang: Error bounds for complementarity problems with tridiagonal nonlinear functions

Nr. 08/12 Tomas Dohnal, Hannes Uecker: Coupled Mode Equations and Gap Solitons for the 2D Gross-Pitaevskii equation with a non-separable periodic potential

Nr. 09/01 Armin Lechleiter, Andreas Rieder: Towards A General Convergence Theory For Inexact Newton Regularizations

Nr. 09/02 Christian Wieners: A geometric data structure for parallel finite elements and the application to multigrid methods with block smoothing

Nr. 09/03 Arne Schneck: Constrained Hardy Space Approximation

Nr. 09/04 Arne Schneck: Constrained Hardy Space Approximation II: Numerics

Nr. 10/01 Ulrich Kulisch, Van Snyder : The Exact Dot Product As Basic Tool For Long Interval Arithmetic

Nr. 10/02 Tobias Jahnke : An Adaptive Wavelet Method for The Chemical Master Equation

Nr. 10/03 Christof Schütte, Tobias Jahnke : Towards Effective Dynamics in Complex Systems by Markov Kernel Approximation

Nr. 10/04 Tobias Jahnke, Tudor Udrescu : Solving chemical master equations by adaptive wavelet compression

Nr. 10/05 Christian Wieners, Barbara Wohlmuth : A Primal-Dual Finite Element Approximation For A Nonlocal Model in Plasticity

Nr. 10/06 Markus Bürg, Willy Dörfler: Convergence of an adaptive hp finite element strategy in higher space-dimensions

Eine aktuelle Liste aller IWRMM-Preprints finden Sie auf:

www.mathematik.uni-karlsruhe.de/iwrmm/seite/preprints

Kontakt

Karlsruher Institut für Technologie (KIT)
Institut für Wissenschaftliches Rechnen
und Mathematische Modellbildung

Prof. Dr. Christian Wieners
Geschäftsführender Direktor

Campus Süd
Engesserstr. 6
76131 Karlsruhe

E-Mail: iwrmm-sekretariat@math.uka.de

www.math.kit.edu/iwrmm/

Herausgeber

Karlsruher Institut für Technologie (KIT)
Kaiserstraße 12 | 76131 Karlsruhe

Juli 2010

www.kit.edu